Antijamming Performance of Space-Frequency Coding in Partial-Band Noise

Celal Eşli, *Student Member, IEEE*, and Hakan Deliç, *Senior Member, IEEE*

***Abstract*—Space-frequency coded (SFC) orthogonal frequency-division multiple access (OFDMA) system is considered under partial band noise jamming (PBNJ). Analytical expressions for the bit error probability (BEP) are derived for OFDMA with and without SFC in a frequency-selective fading environment. It is shown that SFC increases the resistance of OFDMA against PBNJ and reduces the BEP considerably.**

***Index Terms*—Orthogonal frequency-division multiple access (OFDMA), partial band noise jamming (PBNJ), space-frequency coding (SFC).**

I. Introduction

ORTHOGONAL frequency-division multiplexing (OFDM) is an efficient technology that splits the available bandwidth among several closely spaced mutually orthogonal subcarriers. The frequency-selective fading problem commonly encountered in wideband communications is replaced by transmission over multiple flat-fading channels. Nowadays, OFDM is used in terrestrial digital video broadcasting (DVB), wireless local area networks (LANs) such as HIPERLAN/2, 4G systems, high bit rate digital subscriber lines (HDSLs), and asymmetric digital subscriber loops (ADSLs) [17].

Dividing the available subcarrier set among the users gives rise to a multiuser paradigm known as the orthogonal frequency-division multiple access (OFDMA). In the so-called clustered OFDM, each user is assigned a cluster of contiguous subcarriers, which are transmitted over separate antennas so that fading is independent on each cluster [3].

It is conceivable that future-generation tactical communication systems will employ a multicarrier system such as OFDMA for high-rate data transmission [5], [10], [12]. Such systems must not allow various forms of jamming to inhibit the communications between friendly lines. To interfere with the communications, the enemy sends a signal in the form of tones [4], [11] or noise [1], [15], [16], [19] to the receiver at the same frequency band or subband that the transmitter uses. Because the power of the jammer is finite, jamming cannot be applied to the whole band, and the decision as to what portion of the spectrum to attack is a critical problem on the jammer's part. In partial-band noise (PBN) generation, the jammer distributes its total power $J_{\rm tot}$ over T contiguous subbands so that $\alpha = T/N$ of the bandwidth is jammed, where N is the total number of OFDM subbands. The PBN jammer acts as an additive Gaussian noise source with zero-mean, and the effective jamming power spectral density in any subband is $N_j = J_{\rm tot}/W_{\rm tot}$, assuming that $J_{\rm tot}$ is uniformly distributed over entire bandwidth $W_{\rm tot}$.

To ensure that jamming does not hamper communications, appropriate measures need to be taken. For instance, the generalized frequency-hopping (FH) OFDMA system is shown to eliminate narrowband and partial-band interference by careful code design [20]. However, such code designs may leave the system vulnerable to follower jammers, against which pseudo-random hopping is preferred. Moreover, code coordination among the users may not be feasible. Therefore, whether FH is employed or not, other means that add robustness to the tactical communication system are welcome. The use of OFDM offers the possibility of diversity in the frequency domain through space-frequency coding (SFC) [2], [8]. While SFC is intended to provide gains against fading, it is also a proven technique to reduce multiuser interference in FH-OFDMA so long as each user's subcarriers hop independently [6], [7]. Therefore, it is anticipated that SFC should enhance the resistance of an OFDMA system to other forms of interference as well.

In this paper, we consider OFDMA that is equipped with SFC over two transmit antennas and evaluate its performance in the presence of partial band noise jamming (PBNJ) in a frequency-selective fading environment. The premise behind our effort is that there will be instances where the jammer may not hit both subcarriers that are used in SFC, and the postdecoding signal-to-jammer ratio (SJR) will be higher than that experienced by OFDMA alone. Analysis and simulations for various signal-to-noise ratios (SNRs), SJRs, and α values indicate that SFC does indeed provide significant energy efficiency.

The organization of the paper is as follows. Section II briefly outlines the SFC-OFDMA system, including the signal-to-jammer plus noise ratio (SJNR) calculations. Hit probabilities for SFC-OFDMA are computed in Section III. Bit error probability (BEP) performance of OFDMA and SFC-OFDMA is furnished in Section IV. The simulation model and results are in Section V. Conclusions are drawn in Section VI.

Manuscript received January 5, 2005; revised April 5, 2005, June 22, 2005, and August 19, 2005. This work was supported by the Boğaziçi University Research Fund under Grant 04A203. The contents of this paper were presented in the IEEE Military Communications Conference, Atlantic City, NJ, October 2005. The review of this paper was coordinated by Dr. M. Valenti.

C. Eşli was with the Wireless Communications Laboratory, Department of Electrical and Electronics Engineering, Boğaziçi University, Bebek 34342 Istanbul, Turkey. He is now with the Communications Technology Laboratory, Information and Electro-technology Department, ETH Zurich, Zurich 8092, Switzerland (e-mail: cesli@nari.ee.thz.ch).

H. Deliç is with Wireless Communications Laboratory, Department of Electrical and Electronics Engineering, Boğaziçi University, Bebek 34342 Istanbul, Turkey (e-mail: delic@boun.edu.tr).

Digital Object Identifier 10.1109/TVT.2005.863421

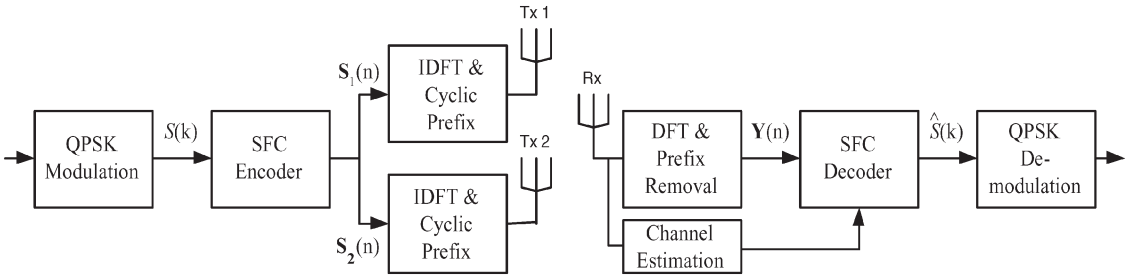

Fig. 1. Block diagram of the SFC-OFDM system. In the figure, $\mathbf{S}_1(n)$ and $\mathbf{S}_2(n)$ are the nth-coded OFDM blocks, and $\mathbf{Y}(n)$ is the corresponding received OFDM block.

II. Space-Frequency Coded (SFC) OFDMA

The block diagram of the OFDM system equipped with SFC capability is given in Fig. 1. The total of N available subcarriers is distributed over $U = N/M$ users, each having M subcarriers that need not be contiguous. User data symbols are modulated with quadrature phase-shift keying (QPSK). Each user's data symbols are fed into a serial-to-parallel converter to generate the nth OFDM block of ith user, which is denoted by

$$\mathbf{s}(i,n) = [S_0(i,n)S_1(i,n)\cdots S_{M-2}(i,n)S_{M-1}(i,n)]^{\mathrm{T}}$$

where $S_m(i,n) := S(i,nM+m),\ m = 0,1,\ldots,M-1,$ is the mth symbol of the nth data block. Using the nth OFDM block $\mathbf{s}(i,n)$, the SF encoder generates the two data vectors [8]

$$\mathbf{s}_1(i,n) = \left[S_0(i,n)\ \ -S_1^*(i,n)\cdots S_{M-2}(i,n)\ \ -S_{M-1}^*(i,n)\right]^{\mathrm{T}},$$
$$\mathbf{s}_2(i,n) = \left[S_1(i,n)\ \ S_0^*(i,n)\cdots S_{M-1}(i,n)\ \ S_{M-2}^*(i,n)\right]^{\mathrm{T}}.$$

We ignore the (i,n) designation for notational simplicity hereafter.

Before transmission, inverse discrete Fourier transform (IDFT) is applied to both vectors and cyclic prefixes appended. Subsequently, $\mathbf{s}_1$ and $\mathbf{s}_2$ are simultaneously transmitted over the respective antennas that are positioned such that the corresponding channels are uncorrelated. IDFT can be implemented through an N-point inverse fast Fourier transform over the N subcarriers by appropriately zero-padding $\mathbf{s}_\ell$, $\ell = 1,2$, to make it an $N \times 1$ vector.

At the receiver, following the cyclic prefix removal, discrete Fourier transform (DFT) is applied. The DFTs of channel impulse responses $h_1 := h_{i,1}(n)$ and $h_2 := h_{i,2}(n)$ observed by the ith user's transmit antennas, which are assumed to stay constant for the duration of the block, have the channel-transfer functions $H_{1,0}, H_{1,1}, \ldots, H_{1,M-1}$ and $H_{2,0}, H_{2,1}, \ldots, H_{2,M-1}$, respectively, at the M subcarriers.

Following OFDM demodulation, the received symbols are

$$\begin{aligned} Y_m &= H_{1,m}S_m + H_{2,m}S_{m+1} + Z_m \\ Y_{m+1}^* &= -H_{1,m+1}^*S_{m+1} + H_{2,m+1}^*S_m + Z_{m+1}^* \end{aligned} \tag{1}$$

for $m = 0,2,4,\ldots,M-2$, where Z_m represents the zero-mean complex additive white Gaussian noise (AWGN) with two-sided power spectral density of $N_0/2$.

Assuming that the channel state information (CSI) is available, the decision estimate

$$\hat{\mathbf{s}} = \mathbf{C}\mathbf{y} \tag{2}$$

is generated through the zero-forcing space-frequency decoder

$$\begin{aligned} \mathbf{C} = &\frac{\left|H_{1,m}H_{1,m+1}^* + H_{2,m}H_{2,m+1}^*\right|}{H_{1,m}H_{1,m+1}^* + H_{2,m}H_{2,m+1}^*} \\ &\times \begin{bmatrix} \left(|H_{1,m+1}|^2+|H_{2,m}|^2\right)^{-\frac{1}{2}} & 0 \\ 0 & \left(|H_{1,m}|^2+|H_{2,m+1}|^2\right)^{-\frac{1}{2}} \end{bmatrix} \\ &\times \begin{bmatrix} H_{1,m+1}^* & H_{2,m} \\ H_{2,m+1}^* & -H_{1,m} \end{bmatrix} \end{aligned} \tag{3}$$

of [18], where $\hat{\mathbf{s}} = [\hat{S}_m\ \hat{S}_{m+1}]^{\mathrm{T}}$ and $\mathbf{y} = [Y_m\ Y_{m+1}^*]^{\mathrm{T}}$. While designing the decoder in [18], a constraint is enforced so as not to change the variance of noise or jammer and leave them as they are in $\mathbf{y}$. From (3), the SFC decoder outputs are

$$\hat{S}_m = \frac{\left|H_{1,m}H_{1,m+1}^* + H_{2,m}H_{2,m+1}^*\right|}{\sqrt{|H_{1,m+1}|^2 + |H_{2,m}|^2}}S_m + \bar{Z}_m \tag{4}$$

$$\hat{S}_{m+1} = \frac{\left|H_{1,m}H_{1,m+1}^* + H_{2,m}H_{2,m+1}^*\right|}{\sqrt{|H_{1,m}|^2 + |H_{2,m+1}|^2}}S_{m+1} + \bar{Z}_{m+1}^* \tag{5}$$

where the post-decoding noise term $\bar{Z}_m(\bar{Z}_{m+1})$ is conditionally Gaussian with the same variance as $Z_m(Z_{m+1})$ for $m = 0,2,4,\ldots,M-2$.

In the absence of the jammer, the SJNRs observed at the SFC decoder output are simply

$$\begin{aligned} \gamma_m^0 &= \frac{\left|H_{1,m}H_{1,m+1}^* + H_{2,m}H_{2,m+1}^*\right|^2}{|H_{1,m+1}|^2 + |H_{2,m}|^2} \cdot \frac{E_s}{N_0} \\ \gamma_{m+1}^0 &= \frac{\left|H_{1,m}H_{1,m+1}^* + H_{2,m}H_{2,m+1}^*\right|^2}{|H_{1,m}|^2 + |H_{2,m+1}|^2} \cdot \frac{E_s}{N_0} \end{aligned} \tag{6}$$

where E_s is the symbol energy, and γ_m^0 is the SJNR at the decoder output for the unjammed subcarrier m.

Assuming that the neighboring subcarriers have the same channel transfer functions, i.e., $H_{1,m} \approx H_{1,m+1}$ and $H_{2,m} \approx H_{2,m+1}$, the SJNRs reduce to

$$\gamma_m^0 \approx \gamma_{m+1}^0 \approx \left(|H_{1,m}|^2 + |H_{2,m}|^2\right) \frac{E_s}{N_0}. \tag{7}$$

To check for the validity of the above assumption, the correlation between adjacent carriers should be taken into account in the analysis. Defining ρ as the correlation coefficient between the channel-transfer functions of the adjacent subcarriers, the random variables $\epsilon_1 = (H_{1,m} - \rho H_{1,m+1})/(\sqrt{1-\rho^2})$ and $\epsilon_2 = (H_{2,m+1} - \rho H_{2,m})/(\sqrt{1-\rho^2})$ are introduced in [18]. By inserting ϵ_1 and ϵ_2 in (6), we can express γ_m^0 and γ_{m+1}^0 as

$$\gamma_m^0 = \left| \rho \sqrt{|H_{1,m+1}|^2 + |H_{2,m}|^2} + \sqrt{1-\rho^2} \frac{H_{1,m+1}^* \epsilon_1 + H_{2,m}^* \epsilon_2^*}{\sqrt{|H_{1,m+1}|^2 + |H_{2,m}|^2}} \right|^2 \frac{E_s}{N_0} \tag{8}$$

$$\gamma_{m+1}^0 = \left| \rho \sqrt{|H_{1,m}|^2 + |H_{2,m+1}|^2} + \sqrt{1-\rho^2} \frac{H_{1,m} \epsilon_1^* + H_{2,m+1}^* \epsilon_2}{\sqrt{|H_{1,m}|^2 + |H_{2,m+1}|^2}} \right|^2 \frac{E_s}{N_0}. \tag{9}$$

The jammer chooses T contiguous subcarriers and distributes its total power over them. Hence, each subcarrier pair in SFC is either subject to a double hit, a single hit, or no hit. Since each symbol is sent on two distinct subcarriers in SFC, there will be cases in which a symbol jammed in one subcarrier is not jammed in the other one. To consider the effects of jamming on the SJNRs at the SF decoder, three distinct hit scenarios should be examined in terms of subcarrier pairs involved in SFC.

1) None of the subcarriers is hit by the jammer.
2) A single subcarrier is hit by the jammer.
3) Both subcarriers are hit by the jammer.

Throughout the rest of the analysis, the SJNR of the subcarrier m subject to a single hit and a double hit is represented by γ_m^1 and γ_m^2, respectively. The first case is already investigated in (8) and (9).

In the second scenario, since one of the subcarriers (say the first one) is hit by the jammer, the received symbols are

$$\begin{aligned} Y_m &= H_{1,m} S_m + H_{2,m} S_{m+1} + G_m J_m + Z_m \\ Y_{m+1}^* &= -H_{1,m+1}^* S_{m+1} + H_{2,m+1}^* S_m + Z_{m+1}^* \end{aligned} \tag{10}$$

where J_m and G_m represent the jamming signal following OFDM demodulation and the channel-transfer function experienced by the jammer, respectively. The SF decoder generates the decision estimates through (3), and therefore, the SJNR at the SF decoder output is found in (11), shown at the bottom of the page, where $N_J = N_j/\alpha$ is the power spectral density of the jammer in a jammed subcarrier.

Finally, when both of the carriers are hit by the jammer, received symbols are observed as

$$\begin{aligned} Y_m &= H_{1,m} S_m + H_{2,m} S_{m+1} + G_m J_m + Z_m \\ Y_{m+1}^* &= -H_{1,m+1}^* S_{m+1} + H_{2,m+1}^* S_m \\ &\quad + G_{m+1}^* J_{m+1}^* + Z_{m+1}^*. \end{aligned} \tag{12}$$

Similar to the second scenario, when both subcarriers are hit the SJNRs at the decoder output are found to be as in (13), shown at the bottom of the page.

$$\gamma_m^1 = \frac{\left| \rho \sqrt{|H_{1,m+1}|^2 + |H_{2,m}|^2} + \sqrt{1-\rho^2} \frac{H_{1,m+1}^* \epsilon_1 + H_{2,m}^* \epsilon_2^*}{\sqrt{|H_{1,m+1}|^2 + |H_{2,m}|^2}} \right|^2 E_s}{N_0 + |G_m|^2 N_J}$$

$$\gamma_{m+1}^1 = \frac{\left| \rho \sqrt{|H_{1,m}|^2 + |H_{2,m+1}|^2} + \sqrt{1-\rho^2} \frac{H_{1,m} \epsilon_1^* + H_{2,m+1}^* \epsilon_2}{\sqrt{|H_{1,m}|^2 + |H_{2,m+1}|^2}} \right|^2 E_s}{N_0 + |G_m|^2 N_J} \tag{11}$$

$$\gamma_m^2 = \frac{\left| \rho \sqrt{|H_{1,m+1}|^2 + |H_{2,m}|^2} + \sqrt{1-\rho^2} \frac{H_{1,m+1}^* \epsilon_1 + H_{2,m}^* \epsilon_2^*}{\sqrt{|H_{1,m+1}|^2 + |H_{2,m}|^2}} \right|^2 E_s}{N_0 + \left(|G_m|^2 + |G_{m+1}|^2\right) N_J}$$

$$\gamma_{m+1}^2 = \frac{\left| \rho \sqrt{|H_{1,m}|^2 + |H_{2,m+1}|^2} + \sqrt{1-\rho^2} \frac{H_{1,m} \epsilon_1^* + H_{2,m+1}^* \epsilon_2}{\sqrt{|H_{1,m}|^2 + |H_{2,m+1}|^2}} \right|^2 E_s}{N_0 + \left(|G_m|^2 + |G_{m+1}|^2\right) N_J} \tag{13}$$

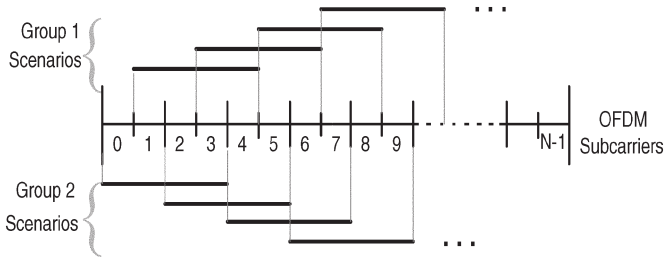

Fig. 2. Separation of possible jamming scenarios into two groups.

III. Computation of Hit Probabilities

Consider an SFC system with two TX antennas so that there are $N/2$ carrier pairs in total for users. It is assumed that each user transmits over $M/2$ pairs of contiguous subcarriers. On the other hand, T of N possible subcarriers is jammed by PBN. Each subcarrier pair is either subject to a double hit, a single hit, or no hit.

1) Subcarrier Pairs Subject to a Double Hit: Jammer chooses T contiguous carriers out of N so that there are $N-T+1$ possible jamming scenarios. Since T is assumed to be even throughout this paper, possible jamming scenarios can be divided into two groups: one consisting of carrier sequences starting from odd-numbered subcarriers and the other starting from even-numbered subcarriers. This separation of possible scenarios is necessary for the ease of derivations. The separation scheme is illustrated in Fig. 2. The first group consists of $\lceil (N-T+1)/2 \rceil$ sequences, whereas the second one consists of $\lfloor (N-T+1)/2 \rfloor$ sequences.

Considering the first group, the probability that d pairs are subject to a double hit is $\prod_{k=0}^{d-1}((T/2-k)/(N/2-k))$. Given d double-hit pairs, the remaining $M/2-d$ pairs are hit-free, with probability $\prod_{m=0}^{M/2-d-1}((N/2-T/2-m)/(N/2-d-m))$. Finally, noting that there are $((M/2)!/d!(M/2-d)!)$ possible cases, the probability that d pairs are subject to a double hit for the first group is

$$P_{\mathrm{dh},1}(d) = \frac{\left\lceil \frac{(N-T+1)}{2} \right\rceil}{N-T+1} \left(\frac{\left(\frac{M}{2}\right)!}{d!\left(\frac{M}{2}-d\right)!} \right) \times \prod_{k=0}^{d-1} \left(\frac{\frac{T}{2}-k}{\frac{N}{2}-k} \right) \prod_{m=0}^{\frac{M}{2}-d-1} \left(\frac{\frac{N}{2}-\frac{T}{2}-m}{\frac{N}{2}-d-m} \right). \quad (14)$$

For the second group, the probability that d pairs are subject to a double hit is $\prod_{k=0}^{d-1}((T/2-1-k)/(N/2-k))$. Given d double-hit pairs, the remaining $M/2-d$ pairs are either hit free or subject to a single hit. Thus, $\prod_{n=0}^{s-1}((2-n)/(N/2-d-n))$ is the probability of observing s single-hit pairs given that there are d double-hit pairs, where s ranges from 0 to $\min(2, M/2-d)$. Next, the remaining $M/2-d-s$ pairs are hit free with the probability $\prod_{m=0}^{M/2-d-s-1}((N/2-T/2-m-1)/(N/2-d-s-m))$. Putting all the above calculations together and recalling that there are $((M/2)!/d!s!(M/2-d-s)!)$ possible cases, the probability that d pairs are subject to double hit for the second group is

$$P_{\mathrm{dh},2}(d) = \frac{\left\lfloor \frac{(N-T+1)}{2} \right\rfloor}{N-T+1} \prod_{k=0}^{d-1} \left(\frac{\frac{T}{2}-k-1}{\frac{N}{2}-k} \right) \times \sum_{s=0}^{\min\left(2,\frac{M}{2}-d\right)} \left[\left(\frac{\left(\frac{M}{2}\right)!}{d!s!\left(\frac{M}{2}-d-s\right)!} \right) \prod_{n=0}^{s-1} \left(\frac{2-n}{\frac{N}{2}-d-n} \right) \times \prod_{m=0}^{\frac{M}{2}-d-s-1} \left(\frac{\frac{N}{2}-\frac{T}{2}-m-1}{\frac{N}{2}-d-m} \right) \right]. \quad (15)$$

where here and in the sequel it is supposed that $\prod_{n=0}^{s-1} f(n) = 1$.

Combining the probabilities for both groups, the exact probability that d pairs are subject to a double hit is found to be $P_{\mathrm{dh}}(d) = P_{\mathrm{dh},1}(d) + P_{\mathrm{dh},2}(d)$. The expected number of subcarrier pairs with a double hit is

$$E[d] = \sum_{d=1}^{\left\lfloor \min\left(\frac{M}{2},\frac{T}{2}\right) \right\rfloor} d P_{\mathrm{dh}}(d). \quad (16)$$

Finally, the probability that any subcarrier pair experiences a double hit is

$$\mathcal{P}_2 = \frac{E[d]}{\frac{M}{2}}. \quad (17)$$

2) Subcarrier Pairs Subject to a Single Hit: Separating the possible jammed-carrier sequences into two groups is also useful for this case. If the first group is considered, it is noticed that there can be no single-hit pair with this group's jamming scenarios. On the other hand, for the second group, $\prod_{k=0}^{s-1}((2-k)/(N/2-k))$ is the probability of observing s pairs subject to a single hit, where s can be 2 at most. Given that there are s single-hit pairs, the remaining $M/2-s$ pairs are hit-free or subject to double hits. Therefore, given that there are s single-hit pairs, the probability of observing d double-hit pairs is $\prod_{n=0}^{d-1}((T/2-n-1)/(N/2-s-n))$, where d ranges from 0 to $\lfloor \min(M/2-s, T/2-1) \rfloor$. Next, $\prod_{m=0}^{M/2-s-d-1}((M/2-T/2-m-1)/(N/2-s-d-m))$ corresponds to the probability of observing $M/2-s-d$ hit-free pairs. Noting that there are $((M/2)!/d!s!(M/2-d-s)!)$ possible different cases, the resulting probability of observing s single-hit pairs is obtained as

$$P_{\mathrm{sh}}(s) = \frac{\left\lfloor \frac{(N-T+1)}{2} \right\rfloor}{N-T+1} \prod_{k=0}^{s-1} \left(\frac{2-k}{\frac{N}{2}-k} \right) \times \sum_{d=0}^{\min\left(\frac{T}{2}-1,\frac{M}{2}-s\right)} \left[\left(\frac{\left(\frac{M}{2}\right)!}{d!s!\left(\frac{M}{2}-d-s\right)!} \right) \prod_{n=0}^{d-1} \left(\frac{\frac{T}{2}-n-1}{\frac{N}{2}-s-n} \right) \times \prod_{m=0}^{\frac{M}{2}-s-d-1} \left(\frac{\frac{N}{2}-\frac{T}{2}-m-1}{\frac{N}{2}-d-s-m} \right) \right]. \quad (18)$$

The expected number of carrier pairs subject to a single hit is

$$E[s] = \sum_{s=1}^{2} sP_{\rm sh}(s) \tag{19}$$

and consequently, any given subcarrier pair experiences a single hit with probability

$$\mathcal{P}_1 = \frac{E[s]}{\frac{M}{2}}. \tag{20}$$

IV. BEP Performance Under PBN Jamming

A. OFDMA

The jammer chooses T contiguous subcarriers from the total of N and distributes its available power $J_{\rm tot}$ evenly over these. Assuming that the jammer's PBN is independent of the background additive Gaussian noise, the powers can be summed to represent the total noise power at the receiver as in [15]. Hence, the average BEP of QPSK modulation under PBNJ is

$$P_b(\gamma_J) = Q(\sqrt{\gamma_J}) \tag{21}$$

where $\gamma_J = E_s/(N_0 + N_J)$ is the average SJNR, and $Q(x) = (1/2\pi)\int_x^\infty \mathrm{e}^{-y^2/2}dy$ [14].

In the OFDMA system, each user transmits over M subcarriers, which are assigned such that collisions are avoided. The BEP of the OFDMA system without jamming averaged over all users can be written as

$$P_b^{\rm OFDMA} = \frac{1}{N}\sum_{i=1}^{U}\sum_{k=1}^{M} P_b(\gamma_{i,k}) \tag{22}$$

where $P_b(\gamma_{i,k})$ represents the BEP of the ith user's kth carrier with the OFDM block-long SJNR $\gamma_{i,k}$. Let $\underline{\Lambda}_\ell$ be the vector consisting of the corresponding channel gains of each user's ℓth transmit antenna (e.g., for $M = 2$, $N = 8$, two transmit antenna case, $\underline{\Lambda}_1 = [\mathcal{H}_{1,1,0}\ \mathcal{H}_{2,1,0}\ \mathcal{H}_{3,1,0}\ \mathcal{H}_{4,1,0}]^{\rm T}$, $\underline{\Lambda}_2 = [\mathcal{H}_{1,2,0}\ \mathcal{H}_{2,2,0}\ \mathcal{H}_{3,2,0}\ \mathcal{H}_{4,2,0}]^{\rm T}$ in nth block, where $\mathcal{H}_{i,\ell,k} := [H_{i,\ell,k}\ H_{i,\ell,k+1}]^{\rm T}$ represents the channel-transfer functions of the ith user's ℓth transmit antenna's kth subcarrier pair). Since the double summation in (22) is over all available subcarriers, it can be simplified to

$$P_b^{\rm OFDMA} = \frac{1}{N}\sum_{m=0}^{N-1} P_b(\gamma_m) \tag{23}$$

where $P_b(\gamma_m)$ represents the unjammed BEP of the mth carrier when the block-long SNR is $\gamma_m = \gamma_S|\Lambda_{1,m}|^2$, where $\gamma_S = E_s/N_0$, and $\Lambda_{1,m}$ is the mth element of $\underline{\Lambda}_1$. If α of the total bandwidth is jammed, inserting (21) into (23) gives

$$P_b^{\rm OFDMA} = \frac{1}{N}\left[\sum_{m\in\mathcal{J}} Q\left(\sqrt{\frac{|\Lambda_{1,m}|^2E_s}{N_0+|G_m|^2N_J}}\right) + \sum_{m\in\mathcal{J}'} Q\left(\sqrt{\frac{|\Lambda_{1,m}|^2E_s}{N_0}}\right)\right] \tag{24}$$

where $\mathcal{J}$ and $\mathcal{J}'$ are the index sets of the jammed and unjammed subcarriers, respectively.

For simplification, the following assumption is taken into account in the ensuing calculations.

A1) The jammer signal does not experience a severe fading (e.g., the jammer is close to the transmitter), and therefore $|G_m| = 1$, $m = 0, 1, \ldots, N-1$.

By A1), (24) is simplified to

$$\begin{aligned} P_b^{\rm OFDMA} &= \frac{1}{N}\left[\sum_{m\in\mathcal{J}} Q\left(\sqrt{|\Lambda_{1,m}|^2\gamma_J}\right) + \sum_{m\in\mathcal{J}'} Q\left(\sqrt{|\Lambda_{1,m}|^2\gamma_s}\right)\right] \\ &= \frac{1}{N}\sum_{m=0}^{N-1}\left[\alpha Q\left(\sqrt{|\Lambda_{1,m}|^2\gamma_J}\right) + (1-\alpha)Q\left(\sqrt{|\Lambda_{1,m}|^2\gamma_s}\right)\right]. \end{aligned} \tag{25}$$

Considering a Rayleigh fading channel, the expected BEP is

$$\bar{P}_b^{\rm OFDMA} = \int_0^\infty \cdots \int_0^\infty P_b^{\rm OFDMA} p(\underline{\gamma})d\underline{\gamma} \tag{26}$$

where $\underline{\gamma} = [\gamma_0\ \gamma_1 \ldots \gamma_{N-1}]^{\rm T}$, and $p(\underline{\gamma})$ is the multivariate Rayleigh probability density function (pdf) that represents the frequency-selective channel gain.

B. SFC-OFDMA

While deriving the BEP of the SFC-OFDMA system, subcarrier pairs should be taken into account. Thus, (23) can be modified as

$$P_b^{\rm SFC-OFDMA} = \frac{1}{N}\left(P_b^0 + P_b^2 + \cdots + P_b^{N-2}\right) \tag{27}$$

where $P_b^m = P_b(\gamma_m) + P_b(\gamma_{m+1})$ represents the total BEP of the contiguous subcarrier pair for $m = 0, 2, \ldots, N-2$. The SJNR changes according to the effect of jamming on the subcarrier pairs. Hence, γ_m can be classified into three types: 1) γ_m^0 representing the hit-free SJNR, i.e., the SNR; 2) γ_m^1 representing the single-hit SJNR; and 3) γ_m^2 representing the double-hit SJNR. Defining $P_b(\gamma_m^i)$, $i = 0, 1, 2$, as the probability of bit error for the given SJNR in the mth carrier, P_b^m can be expressed as the summation of different hit cases (e.g., double hit, single hit, hit-free)

$$\begin{aligned} P_b^m &= \left[\mathcal{P}_2P_b\left(\gamma_m^2\right) + \mathcal{P}_1P_b\left(\gamma_m^1\right) + \mathcal{P}_0P_b\left(\gamma_m^0\right)\right] \\ &\quad + \left[\mathcal{P}_2P_b\left(\gamma_{m+1}^2\right) + \mathcal{P}_1P_b\left(\gamma_{m+1}^1\right) + \mathcal{P}_0P_b\left(\gamma_{m+1}^0\right)\right] \end{aligned} \tag{28}$$

where $\mathcal{P}_1$ and $\mathcal{P}_2$ are defined in Section III, and $\mathcal{P}_0 = 1 - \mathcal{P}_1 - \mathcal{P}_2$. Therefore, $P_b(\gamma_m^0)$ and $P_b(\gamma_{m+1}^0)$ can be found by substituting (8) and (9) into (21) as

$$P_b(\gamma_m^0) = Q\left(\left[\left|\rho\sqrt{|\Lambda_{1,m+1}|^2+|\Lambda_{2,m}|^2} + \sqrt{1-\rho^2}\frac{\Lambda_{1,m+1}^*\epsilon_1+\Lambda_{2,m}^*\epsilon_2^*}{\sqrt{|\Lambda_{1,m+1}|^2+|\Lambda_{2,m}|^2}}\right|^2\frac{E_s}{N_0}\right]^{\frac{1}{2}}\right) \tag{29}$$

$$P_b(\gamma_{m+1}^0) = Q\left(\left[\left|\rho\sqrt{|\Lambda_{1,m}|^2+|\Lambda_{2,m+1}|^2} + \sqrt{1-\rho^2}\frac{\Lambda_{1,m}\epsilon_1^*+\Lambda_{2,m+1}^*\epsilon_2}{\sqrt{|\Lambda_{1,m}|^2+|\Lambda_{2,m+1}|^2}}\right|^2\frac{E_s}{N_0}\right]^{\frac{1}{2}}\right) \tag{30}$$

for $m = 0, 2, \ldots, N-1$. Similarly, $P_b(\gamma_m^1)$ and $P_b(\gamma_{m+1}^1)$ can be found in a similar fashion by substituting (11) into (21) as

$$P_b\left(\gamma_m^1\right) = Q\left(\left[\left|\rho\sqrt{|\Lambda_{1,m+1}|^2+|\Lambda_{2,m}|^2} + \sqrt{1-\rho^2} \times \frac{\Lambda_{1,m+1}^*\epsilon_1+\Lambda_{2,m}^*\epsilon_2^*}{\sqrt{|\Lambda_{1,m+1}|^2+|\Lambda_{2,m}|^2}}\right|^2\frac{E_s}{N_0+|G_m|^2N_J}\right]^{\frac{1}{2}}\right) \tag{31}$$

$$P_b\left(\gamma_{m+1}^1\right) = Q\left(\left[\left|\rho\sqrt{|\Lambda_{1,m}|^2+|\Lambda_{2,m+1}|^2} + \sqrt{1-\rho^2} \times \frac{\Lambda_{1,m}\epsilon_1^*+\Lambda_{2,m+1}^*\epsilon_2}{\sqrt{|\Lambda_{1,m}|^2+|\Lambda_{2,m+1}|^2}}\right|^2\frac{E_s}{N_0+|G_m|^2N_J}\right]^{\frac{1}{2}}\right). \tag{32}$$

Last, $P_b(\gamma_m^2)$ and $P_b(\gamma_{m+1}^2)$ are expressed by substituting (13) into (21) as

$$P_b(\gamma_m^2) = Q\left(\left[\left|\rho\sqrt{|\Lambda_{1,m+1}|^2+|\Lambda_{2,m}|^2} + \sqrt{1-\rho^2}\frac{\Lambda_{1,m+1}^*\epsilon_1+\Lambda_{2,m}^*\epsilon_2^*}{\sqrt{|\Lambda_{1,m+1}|^2+|\Lambda_{2,m}|^2}}\right|^2 \times \frac{E_s}{N_0+\left(|G_m|^2+|G_{m+1}|^2\right)N_J}\right]^{\frac{1}{2}}\right) \tag{33}$$

$$P_b(\gamma_{m+1}^2) = Q\left(\left[\left|\rho\sqrt{|\Lambda_{1,m}|^2+|\Lambda_{2,m+1}|^2} + \sqrt{1-\rho^2}\frac{\Lambda_{1,m}\epsilon_1^*+\Lambda_{2,m+1}^*\epsilon_2}{\sqrt{|\Lambda_{1,m}|^2+|\Lambda_{2,m+1}|^2}}\right|^2 \times \frac{E_s}{N_0+\left(|G_m|^2+|G_{m+1}|^2\right)N_J}\right]^{\frac{1}{2}}\right). \tag{34}$$

In the ensuing derivations, $|G_m| = |G_{m+1}| = 1$ will be assumed by (A1).

The average BEP of SFC-OFDMA over a Rayleigh fading channel is

$$\bar{P}_b^{\mathrm{SFC-OFDMA}} = \int_0^\infty \cdots \int_0^\infty P_b^{\mathrm{SFC-OFDMA}} p(\underline{\gamma_1}) p(\underline{\gamma_2}) d\underline{\gamma_1} d\underline{\gamma_2} \tag{35}$$

where $p(\underline{\gamma_1})$ and $p(\underline{\gamma_2})$ are multivariate Rayleigh pdfs for the channels experienced by the two transmit antennas, respectively. By inserting (27) in (35), we obtain

$$\bar{P}_b^{\mathrm{SFC-OFDMA}} = \frac{1}{N}\int_0^\infty \cdots \int_0^\infty \left(P_b^0 + P_b^2 + \cdots + P_b^{N-2}\right) p(\underline{\gamma_1}) p(\underline{\gamma_2}) d\underline{\gamma_1} d\underline{\gamma_2} \tag{36}$$

where $\underline{\gamma_i} = [\gamma_{i,0}\ \gamma_{i,1} \cdots \gamma_{i,N-1}]^{\mathrm{T}}$, and $\gamma_{i,m}$ represents the ith antenna's mth subcarrier for $i = 1, 2$. Since P_b^m are summed, the integral can be taken separately for each P_b^m. Focusing on the integral of P_b^0, we make the following assumption in addition to A1).

A2) Per user, the channel gains of the space-frequency coded subcarrier pairs are mutually uncorrelated.

This is particularly justifiable when the subcarrier pairs are not contiguous and because only $M < N$ subcarriers are assigned per user. Moreover, distinct users communicate over uncorrelated channels. By (A2), we can conclude that each subcarrier pair is independent of the others because $\underline{\Lambda}_\ell$ consists of uncorrelated channel gains. Then, putting (28) in (36), we get

$$\begin{aligned} P_b^0 = \frac{1}{N}\int_0^\infty \cdots \int_0^\infty & \left[\mathcal{P}_2\left(P_b(\gamma_0^2)+P_b(\gamma_1^2)\right)+\mathcal{P}_1\left(P_b(\gamma_0^1)+P_b(\gamma_1^1)\right)\right. \\ & \left. +\mathcal{P}_0\left(P_b(\gamma_0^0)+P_b(\gamma_1^0)\right)\right] \\ & \times p_1(\underline{\nu}_0)p_2(\underline{\nu}_0)p_1(\underline{\nu}_2)p_2(\underline{\nu}_2) \\ & \cdots p_1(\underline{\nu}_{N-2})p_2(\underline{\nu}_{N-2})d\underline{\gamma_1}d\underline{\gamma_2} \end{aligned}$$

and this simplifies to

$$\begin{aligned} P_b^0 = \frac{1}{N}\int_0^\infty\int_0^\infty\int_0^\infty\int_0^\infty & \left[\mathcal{P}_2\left(P_b(\gamma_0^2)+P_b(\gamma_1^2)\right)+\mathcal{P}_1\left(P_b(\gamma_0^1)+P_b(\gamma_1^1)\right)\right. \\ & \left. +\mathcal{P}_0\left(P_b(\gamma_0^0)+P_b(\gamma_1^0)\right)\right] p_1(\underline{\nu}_0)p_2(\underline{\nu}_0) \\ & \times d\gamma_{1,0}d\gamma_{2,0}d\gamma_{1,1}d\gamma_{2,1} \end{aligned} \tag{37}$$

where $\underline{\nu}_m = [\gamma_m \ \ \gamma_{m+1}]^{\mathrm{T}}$ and $p_i(\underline{\nu}_m)$, $i = 1, 2$, is the bivariate Rayleigh pdf for the adjacent subcarriers.

Define the two random variables u_1 and u_2 as

$$\begin{aligned} u_1 = & \left|\rho\sqrt{|\Lambda_{1,m+1}|^2+|\Lambda_{2,m}|^2}\right. \\ & \left. +\sqrt{1-\rho^2}\frac{\Lambda_{1,m+1}^*\epsilon_1+\Lambda_{2,m}^*\epsilon_2^*}{\sqrt{|\Lambda_{1,m+1}|^2+|\Lambda_{2,m}|^2}}\right|^2\gamma_J \\ u_2 = & \left|\rho\sqrt{|\Lambda_{1,m}|^2+|\Lambda_{2,m+1}|^2}\right. \\ & \left. +\sqrt{1-\rho^2}\frac{\Lambda_{1,m}\epsilon_1^*+\Lambda_{2,m+1}^*\epsilon_2}{\sqrt{|\Lambda_{1,m}|^2+|\Lambda_{2,m+1}|^2}}\right|^2\gamma_J \end{aligned} \tag{38}$$

where γ_J is the average SJNR. The pdf of u_i is [18]

$$p_{u_i}(u_i) = \left(\frac{1-\rho^2}{\gamma_J}+\frac{\rho^2}{\gamma_J^2}u_i\right)e^{-\frac{u_i}{\gamma_J}} \tag{39}$$

for $i = 1, 2$. Then, (37) leads to the following expression by substituting (29)–(34) into (37) and rearranging:

$$\begin{aligned} P_b^0 = \frac{1}{N}\Bigg[& \mathcal{P}_2\left(\int_0^\infty Q(\sqrt{u_1})p_{u_1}(u_1)du_1\right. \\ & \left.+\int_0^\infty Q(\sqrt{u_2})p_{u_2}(u_2)du_2\right)\Bigg|_{\gamma_J=\frac{E_s}{N_0+2N_J}} \\ & +\mathcal{P}_1\left(\int_0^\infty Q(\sqrt{u_1})p_{u_1}(u_1)du_1\right. \\ & \left.+\int_0^\infty Q(\sqrt{u_2})p_{u_2}(u_2)du_2\right)\Bigg|_{\gamma_J=\frac{E_s}{N_0+N_J}} \\ & +\mathcal{P}_0\left(\int_0^\infty Q(\sqrt{u_1})p_{u_1}(u_1)du_1\right. \\ & \left.+\int_0^\infty Q(\sqrt{u_2})p_{u_2}(u_2)du_2\right)\Bigg|_{\gamma_J=\frac{E_s}{N_0}}\Bigg]. \end{aligned}$$

After taking the integrals, P_b^0 simplifies to

$$\begin{aligned} P_b^0 = \frac{1}{N}\Bigg[& \mathcal{P}_2\Psi\left(\frac{E_s}{N_0+2N_J}\right) \\ & +\mathcal{P}_1\Psi\left(\frac{E_s}{N_0+N_J}\right)+\mathcal{P}_0\Psi\left(\frac{E_s}{N_0}\right)\Bigg] \end{aligned} \tag{40}$$

where the function $\Psi(x)$ is

$$\Psi(x) = \frac{-2\sqrt{x}+2\sqrt{x+2}-x^{\frac{3}{2}}+x\sqrt{x+2}-\sqrt{x}\rho^2}{(x+2)^{\frac{3}{2}}}.$$

Finally, if P_b^m for $m = 2, 4, \ldots, N-2$ is derived in a similar fashion as P_b^0, the resulting average BEP of SFC-OFDMA system over a Rayleigh fading channel is reduced to a closed form. Noticing that P_b^0 is independent of m, we can conclude that P_b^m is the same for all m. Thus, the average BEP of SFC-OFDMA system is

$$\bar{P}_b^{\mathrm{SFC-OFDMA}} = \frac{N}{2}P_b^0. \tag{41}$$

For fixed E_b/N_0 and E_b/N_j, if the number of jammed carriers increases, it will lead $\mathcal{P}_2$ to increase, whereas $\mathcal{P}_0$ will decrease. On the other hand, because increasing α reduces N_J, there will be a tradeoff between α and N_J. Through this tradeoff, the jammer can find an optimum $\alpha = \alpha^*$, where (41) reaches its maximum, and this α is the worst-case jamming scenario for the actual transmitter–receiver. Because the solution

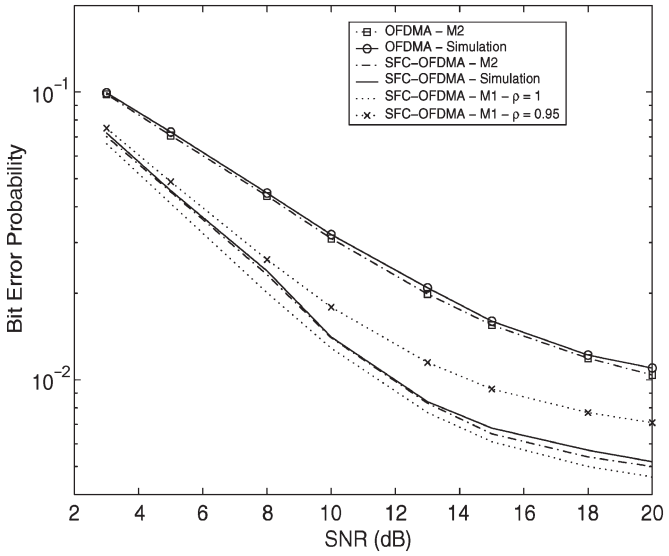

Fig. 3. BEP versus SNR for OFDMA with 16 users in PBNJ and frequency-selective fading (two TX antennas for SFC-OFDMA, $N = 64$, $M = 4$, SJR $= 15$ dB, $\alpha = 0.5$, QPSK modulation).

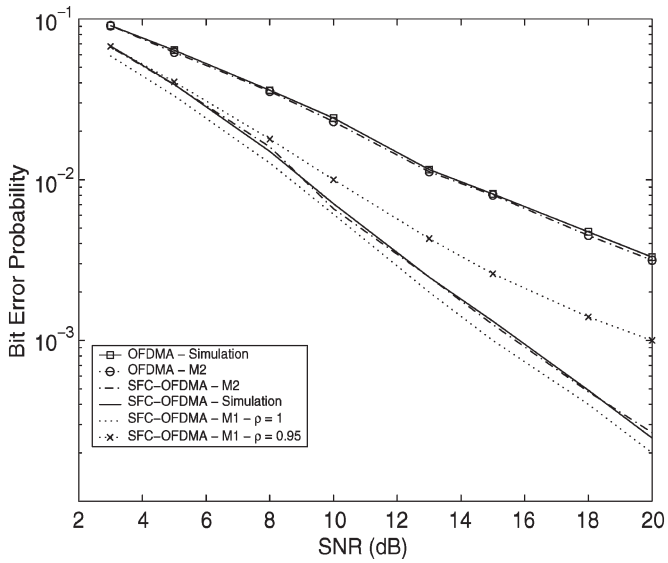

Fig. 4. BEP versus SNR for OFDMA with 16 users in PBNJ and frequency-selective fading (two TX for SFC-OFDMA, $N = 64$, $M = 4$, SJR $= 25$ dB, $\alpha = 0.5$, QPSK modulation).

for α^* involves both α and T, the theoretical analysis here is not trivial.

It should also be noted that jamming contiguous bands as PBNJ does causes the double hits to occur more frequently than single hits, because the contiguous jamming scenario prevents the expected number of single-hit pairs to exceed two as mentioned in Section III. Thus, double-hit occurrences become more dominant.

V. Numerical Evaluations and Simulations

The SF block coding scheme shown in Fig. 1 is adopted and the performance of OFDMA system with and without SFC is tested in the presence of PBNJ. There are $N = 64$ available subcarriers in total and $M = 4$ to support 16 users. The jammer interferes with subcarriers, which are randomly selected at each OFDM block. Symbols with QPSK modulation are transmitted over frequency-selective channels modeled as finite impulse response (FIR) filters and contaminated by zero-mean complex AWGN. The FIR structures are of order five with complex Gaussian-distributed coefficients and flat power delay profile. The channels experienced by each antenna are assumed to be uncorrelated, and CSI is perfectly known at the receiver. All simulations operate at the baseband, and channel coding is not applied. The cyclic prefix length is set to six symbols. The bit error rate (BER) results reflect the averages of 1000 independent channel pair realizations. We define the SNR as SNR $= E_b/N_0$ and the SJR as SJR $= E_b/N_j$. In case of SFC, the symbol energies are shared by the two transmit antennas.

The average error probabilities are determined through three methods.

M1) The expectation given by (40) and (41) is calculated.

M2) The error probabilities in (29)–(34), which are computed for individual channel realizations, are inserted in (27) and (28) and then averaged.

M3) Simulations.

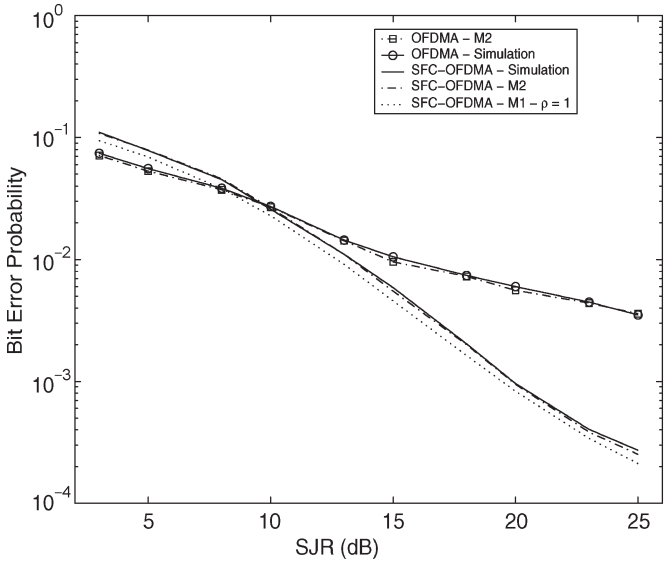

Fig. 5. BEP versus SJR for OFDMA with 16 users in PBNJ and frequency-selective fading (two TX antennas for SFC-OFDMA, $N = 64$, $M = 4$, SNR $= 20$ dB, $\alpha = 0.5$, QPSK modulation).

In the ensuing evaluations, the results obtained from these methods are in remarkable agreement.

Figs. 3 and 4 depict that at high SNRs, the performance limiting factor is PBNJ. The OFDMA performance under PBN is remarkably close to its no-jamming BEP, especially at low SNRs for SJR $= 15$ dB (Fig. 3), and at medium-to-high SNR range for SJR $= 25$ dB (Fig. 4). This outcome supports the reports in [9] and [10] that multicarrier transmission is resistant to PBNJ. At high SJR and SNR, the diversity gain offered by SFC becomes noticeable. For a BEP of 1×10^{-2} at SJR $=$ 25 dB, the OFDMA system with SFC requires about 6 dB less energy to combat noise compared to OFDMA alone.

Fig. 5 shows the BEP performance against SJR for SNR $= 20$ dB. As the SJR increases, the BEP performance is

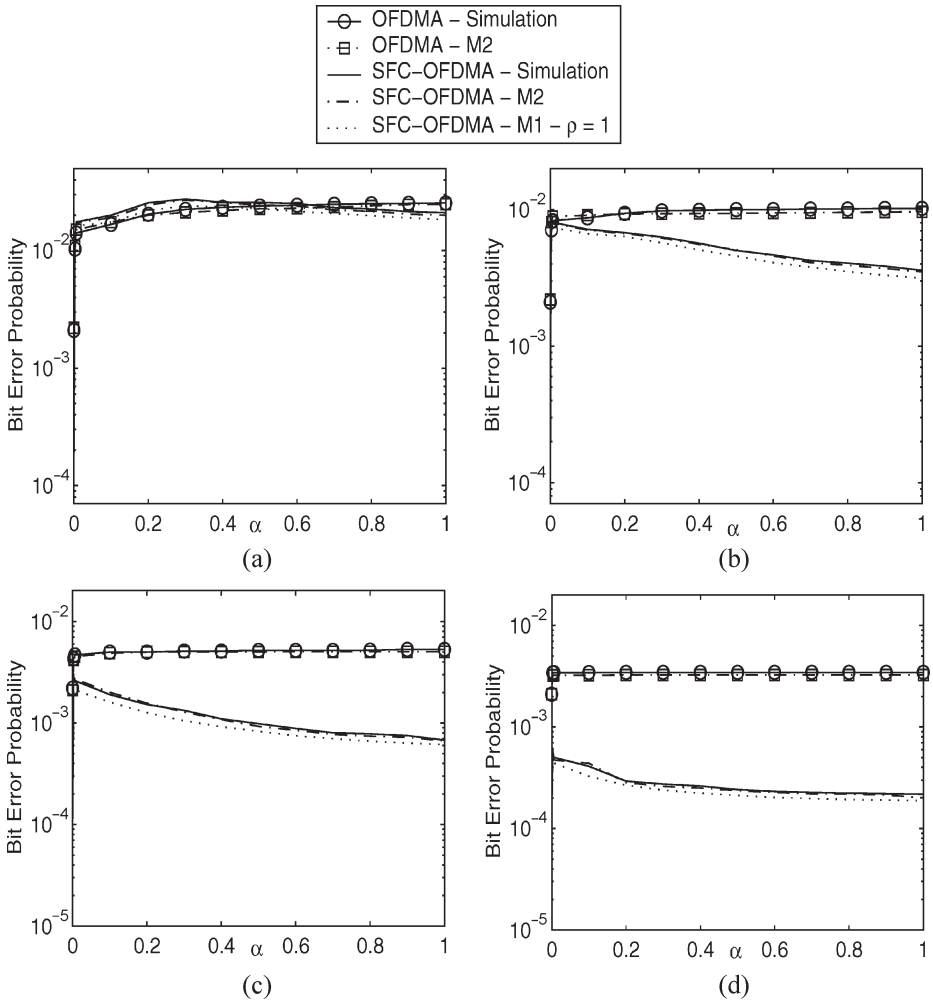

Fig. 6. BEP versus α for OFDMA with 16 users in PBNJ and frequency-selective fading (two TX antennas for SFC-OFDMA, $N = 64$, $M = 4$, SNR $= 20$ dB, QPSK modulation). (a) SJR $= 10$ dB. (b) SJR $= 15$ dB. (c) SJR $= 20$ dB. (d) SJR $= 25$ dB.

augmented, and SFC supplies a 7-dB SJR improvement at a BEP of 5×10^{-3}. The diversity gain kicks in as the SJR grows, which is not suprising because the jammer acts as Gaussian noise. Thus, SNR and SJR play identical roles from the diversity viewpoint. At low SJRs, the double-hit error probabilities in (33) and (34) increase enormously, and this, in conjunction with the fact that $\mathcal{P}_2 > \mathcal{P}_1$ in PBNJ, leads to a slight performance deterioration with SFC.

In all the graphs so far, the expected BEP computation for SFC-OFDMA with $\rho = 1$ is very close to the results obtained from averaging over channel realizations and simulations (note the overshooting with $\rho = 0.95$). This supports the assumption that adjacent subcarriers have almost identical channel-transfer functions.

In Fig. 6, the effect of the fraction of the bandwidth jammed (α) is investigated. Since the total jammer power is fixed, as α increases, the effective power per subcarrier is reduced proportionally. Therefore, the BEP curves reflect the tradeoff between the number of jammed subcarriers versus the PBN power per subcarrier. For SFC-OFDMA at SJR $= 10$ dB, the jammer induces maximum damage at $\alpha^* = 0.3$. Likewise, the worst case jamming occurs at $\alpha^* = 0.06$ for SJR $= 15$ dB, $\alpha^* = 0.03$ for SJR $= 20$ dB, and SJR $= 25$ dB. Thus, SJR and α^* are inversely related for SFC-OFDMA and fixed SNR. The figures also display the full SFC diversity that is present in the absence of PBNJ for $\alpha = 0$. Notice that at low SJR, the diversity gain disappears for $\alpha = \alpha_0 = 2/N$ (note that $N = 64$ here), where the jammed subcarriers are hit with full force, and $\alpha^* \to \alpha_0$ as SJR increases. In addition, Fig. 6 further verifies the performance improvement that is attained for $\alpha > \alpha_0$ as SJR increases.

Although perfect knowledge of CSI is assumed throughout the analyses and simulations, it is conceivable that the pilot subcarriers that assist channel estimation suffer from jamming as well. The resulting performance loss from PBNJ-induced imperfect CSI is analyzed, and equalizer solutions are developed in [13]. Let the channel-estimation errors ζ_n be modeled as independent and identically distributed Gaussian random variables with zero mean. Fig. 7 depicts the performance of SFC-OFDMA in the presence of PBNJ and channel-estimation errors for $E[|\zeta_n|^2]/E[|H_{1,m}|^2] = E[|\zeta_n|^2]/E[|H_{2,m}|^2] = -20$ dB for all m, where $E[\cdot]$ is the expectation operator. Similar levels of BEP degradation are observed for both OFDMA and SFC-OFDMA, and the gain provided by SFC is preserved. At low

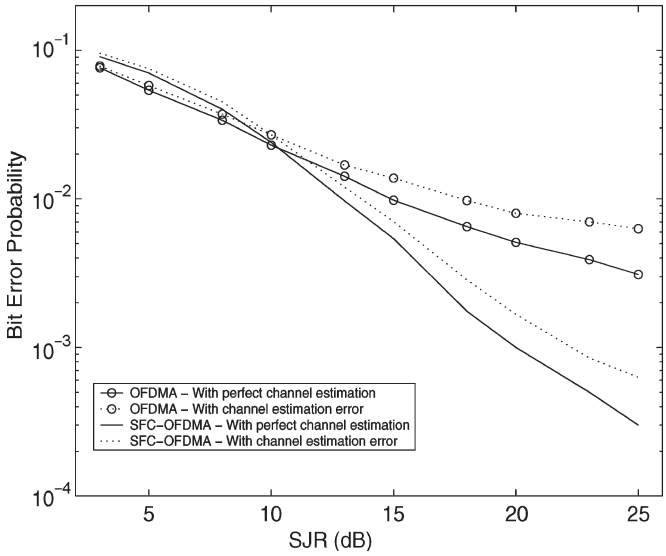

Fig. 7. Simulation results for BEP versus SJR with and without channel-estimation errors (two TX antennas for SFC-OFDMA, $N = 64$, $M = 4$, SNR $= 20$ dB, $\alpha = 0.5$, QPSK modulation).

SJR, the BEP performance is already poor enough, and lack of perfect CSI does not make things much worse.

VI. Conclusion

We have considered possible benefits of employing SFC with zero-forcing decoding against PBNJ in an OFDMA system. BEP analysis has shown that SFC injects significant gains in the medium-to-high SJR range, which is consistent with the behavior of transmit diversity. The influence of SFC on the BEP is related with $J_{\rm tot}$ and α, and the reduction in the BEP relative to OFDMA increases inversely proportional to SJR. Jamming-induced CSI imperfections result in tolerable performance degradation so long as the channel-estimation error variance is sufficiently low.

The performance evaluation is a worst case analysis in the sense that the jammer is not subject to fading. Simulations, where the jammer signal does go through independent fading, show that there might be over two orders of magnitude BEP enhancement at SJR $= 20$ dB for channels with severe nulls. However, the average BEP over 1000 channel realizations is marginally better than the worst case because in general, the jammer's band does not fully overlap with the null, particularly if α is small.

Finally, the BEP performance is invariant to the total number of subcarriers N because the SJR remains constant per subband, if the total signal and jammer energies remain the same.

References

[1] J. S. Bird and E. Felstead, "Antijam performance of fast frequency hopped M-ary NCFSK—An overview," *IEEE J. Sel. Areas Commun.*, vol. SAC-4, no. 2, pp. 216–233, Mar. 1986.

[2] H. Bölcskei and A. J. Paulraj, "Space-frequency coded broadband OFDM systems," in *Proc. IEEE Wireless Communications and Networking Conf.*, Chicago, IL, Sep. 2000, vol. 1, pp. 1–6.

[3] B. Daneshrad, L. Cimini, M. Carloni, and N. Sollenberger, "Performance and implementation of clustered-OFDM for wireless communications," *Mob. Netw. Appl.*, vol. 2, no. 4, pp. 305–314, 1997.

[4] I. A. Ghareeb and A. Yongacoglu, "Performance analysis of frequency hopped/coherent MPSK in the presence of multitone jamming," in *Proc. IEEE Military Communications Conf.*, Fort Monmouth, NJ, Oct. 1994, vol. 3, pp. 821–825.

[5] E. Gunawan and Y. Zhu, "Performance of MC-CDMA system with power balance control over partial-band noise jammed multipath fading channels," in *Proc. IEEE Vehicular Technology Conf.*, Tokyo, Japan, May 2000, vol. 2, pp. 1485–1488.

[6] T. Kurt and H. Deliç, "Collision avoidance in space-frequency coded FH-OFDMA," in *Proc. Rec. IEEE Int. Conf. Communications*, Paris, France, Jun. 2004, vol. 1, pp. 269–273.

[7] ——, "Space-frequency coding reduces the collision rate in FH-OFDMA," *IEEE Trans. Wireless Commun.*, vol. 4, no. 5, pp. 2045–2050, Sep. 2005.

[8] K. Lee and D. B. Williams, "A space-frequency transmitter diversity technique for OFDM systems," in *Proc. IEEE Global Communications Conf.*, San Francisco, CA, Nov. 2000, vol. 3, pp. 1473–1477.

[9] E. Lemois and F. Buda, "New advances in multi-carrier spread spectrum techniques for tactical communications," in *Proc. IEEE Military Communications Conf.*, Boston, MA, Oct. 1998, vol. 2, pp. 664–668.

[10] C. Martin, E. Lemois, F. Buda, and D. Merel, "Description of a complete multi-carrier spread spectrum transmission chain for robust and discreet tactical communications," in *Proc. IEEE Military Communications Conf.*, Los Angeles, CA, Oct. 2000, vol. 2, pp. 942–946.

[11] M. Moeneclaey, M. V. Bladel, and H. Sari, "Sensitivity of multiple-access techniques to narrow-band interference," *IEEE Trans. Commun.*, vol. 49, no. 3, pp. 497–505, Mar. 2001.

[12] J. E. M. Nilsson and T. C. Giles, "Wideband multi-carrier transmission for military HF communication," in *Proc. IEEE Military Communications Conf.*, Monterey, CA, Nov. 1997, vol. 2, pp. 1046–1051.

[13] C. S. Patel, L. Stüber, and T. G. Pratt, "Analysis of OFDM/MC-CDMA under channel estimation and jamming," in *Proc. IEEE Wireless Communications and Networking Conf.*, Atlanta, GA, Mar. 2004, vol. 2, pp. 954–958.

[14] J. G. Proakis, *Digital Communications*, 4th ed. New York: McGraw-Hill, 2001.

[15] M. Simon and A. Polydoros, "Coherent detection of frequency-hopped quadrature modulations in the presence of jamming—Part I: QPSK and QASK modulations," *IEEE Trans. Commun.*, vol. COMM-29, no. 11, pp. 1644–1660, Nov. 1981.

[16] J. Tan and G. L. Stüber, "Anti-jamming performance of multi-carrier spread spectrum with constant envelope," in *Proc. Rec. IEEE Int. Conf. Communications*, Anchorage, AK, May 2003, vol. 1, pp. 743–747.

[17] R. Van Nee and R. Prasad, *OFDM for Wireless Multimedia Communications*. Boston, MA: Artech House, 2000.

[18] A. Vielmon, Y. Li, and J. R. Barry, "Performance of Alamouti transmit diversity over time-varying Rayleigh-fading channels," *IEEE Trans. Wireless Commun.*, vol. 3, no. 3, pp. 1369–1373, Sep. 2004.

[19] H. Zhang and Y. Li, "Anti-jamming property of clustered OFDM for dispersive channels," in *Proc. IEEE Military Communications Conf.*, Boston, MA, Oct. 2003, vol. 1, pp. 336–340.

[20] S. Zhou, G. B. Giannakis, and A. Scaglione, "Long codes for generalized FH-OFDMA through unknown multipath channels," *IEEE Trans. Commun.*, vol. 49, no. 4, pp. 721–733, Apr. 2001.

Celal Eşli (S'03) received the B.S. (with honors) and M.S. degrees in electrical and electronics engineering from Boğaziçi University, Istanbul, Turkey, in 2003 and 2005, respectively. He is currently working toward the Ph.D. degree at the Information and Electro-technology Department, Swiss Federal Institute of Technology (ETHZ), Zurich, Switzerland.

His research interests are in the broad area of wireless communications.

Hakan Deliç (S'88–M'93–SM'00) received the B.S. degree (with honors) in electrical and electronics engineering from Boğaziçi University, Istanbul, Turkey, in 1988, and the M.S. and Ph.D. degrees in electrical engineering from the University of Virginia, Charlottesville, in 1990 and 1992, respectively.

He was a Research Associate with the University of Virginia Health Sciences Center from 1992 to 1994. In September 1994, he joined the University of Southwestern Louisiana, Lafayette, where he was on the faculty of the Department of Electrical and Computer Engineering until February 1996. He was a Visiting Associate Professor in the Department of Electrical and Computer Engineering, University of Minnesota, Minneapolis, during the 2001–2002 academic year. He is currently a professor of electrical and electronics engineering at Boğaziçi University. His research interests lie in the areas of communications and signal processing. His current research focuses on wireless multiple access, application of signal processing techniques to wireless networking, ultrawideband communications, iterative decoding, robust systems, and sensor networks. He frequently serves as a consultant to the telecommunications industry.